VOL. 10, NO. 22, DECEMBER 2015 ISSN 1819-6608
ARPN Journal of Engineering and Applied Sciences


www.arpnjournals.com

EEG-BASED AESTHETICS PREFERENCE MEASUREMENT WITH 3D STIMULI USING WAVELET TRANSFORM

Lin Hou Chew, Jason Teo and James Mountstephens
Faculty of Computing and Informatics, Universiti Malaysia Sabah, Kota Kinabalu, Malaysia
E-Mail: chewqueenie@hotmail.com

ABSTRACT

This study investigates on aesthetics preference measurement of human using electroencephalogram (EEG) for virtual motion 3D shapes. The 3D shapes are generated using the Gielis superformula in bracelet-like shapes. EEG signals were collected by using a wireless medical grade EEG device, B-Alert X10 from Advance Brain Monitoring. Wavelet transforms were used to decompose the signals into 5 different bands, alpha, beta, gamma, delta and theta. Linear Discriminant analysis (LDA) and K-Nearest Neighbor (KNN) were used as classifiers to train and test different combinations of the features. Classification accuracy of up to 82.14% could be obtained using KNN with entropy of beta, gamma, delta and theta rhythms as features from channels Fz, POz and P4.

Keywords: aesthetics preference, electroencephalogram, brain computer interface, wavelet transform, 3-Dimensional design, K-nearest neighbor, linear discriminant analysis.

INTRODUCTION

Aesthetics experience brings across mind pleasure towards humans. Aesthetics is one of the important features in product design and system development where aesthetic products are perceived to have better usability [1].

Aesthetics are often related with emotion. Brown and Dissanayake [2] claim that, aesthetics experiences are closely related with human emotion. Several researchers [3], [4] suggested that human emotion could directly influence aesthetics preference. Some studies have been conducted to recognize human preference on music [5], images [6] and video stimuli [7].

Emotion is an important part of human, where emotion is central of homeostatic life regulating processes, not only for human, but all living creatures [8]. Humans conceive emotion as part of daily life. Numerous studies were conducted to recognize human emotion [9], [10], [11], [12]. The recognition of human emotions enables a better guiding and aiding throughout the experience of using computer machine.

The frontal lobe plays an important role in activities reflect emotions [11], [12], [13]. Wang *et al.* [11] also show that activities in parietal lobe could be related with emotion. Cela-Conde *et al.* [14] claim that the prefrontal cortex is related to aesthetics experiences.

Most of the studies in preference are focused on music, images, and videos. In this study, 3-dimensional (3D) motion stimuli are used to elicit human aesthetics experiences. The literature review on preference extraction on 3-dimensional (3D) is limited. Several researches show that there are differences in brain activities during viewing 2-dimensional (2D) and 3D stimuli [15], [16]. Todd [16] mentioned that perceiving 3D stimuli involve both dorsal and ventral pathways, where the dorsal pathway involves the occipital and parietal lobe, while the ventral pathway involves the median temporal lobe and dorsal pathway.

The challenges in recognizing aesthetic preference is that aesthetic experiences are not always conscious, aesthetic experiences turn into the conscious when the aesthetic experience is extreme [17], whereas [4] suggested that there is an unconscious rule when selecting the preference.

In this study, an electroencephalogram (EEG) device is used to acquire human brain activities during viewing 3D stimuli, the acquired signals then undergoes processing and feature extraction to obtain important features. The features are used to train two types of classifiers. The Linear Discriminant Analysis (LDA) and K-Nearest Neighbor (KNN) methods are used to classify the features into 2 classes, like and dislike to indicate the preference.

DATA ACQUISITION

The detail information on acquisition process is as shown in Figure-1.

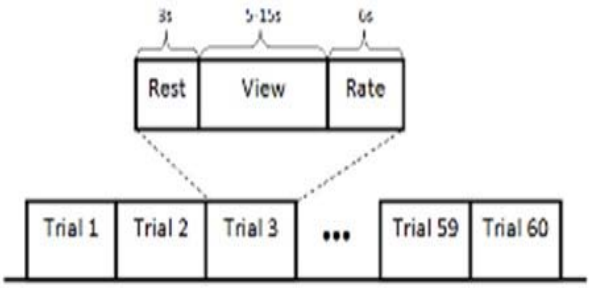

Figure-1. The detail on acquisition process.

In each trial, there are 3 main states, resting, viewing and rating state. During resting state, a blank screen is displayed to subject for 3 seconds to avoid any brain activities related to previous trial.

During viewing state, a 3D motion shape is displayed to subject. The shape is moving in a rotating way to enable subjects in viewing the shapes from different angles. The shape is displayed at a minimum of 5 seconds and a maximum of 15 seconds, whereby the time

of viewing is decided by the subject. A minimum of 5 seconds are compulsory for all shapes, the subject are free to proceed to next state after 5 seconds. However, after the maximum time of 15 seconds, the system will automatically proceed to the next state. The decision of allowing the subject on deciding the viewing time is to reduce subject waiting time as well as reduce fatigue level of subject. Numerous studies reported that Interactive Evolutionary Computation (IEC) caused fatigue on subjects [18]. The subject is required to complete a monotonous and repetitive task during the experiment which caused the subject to get bored [19] and further leads to fatigue [20].

Rating state is displayed to user for 6 seconds. In this state, a 5-point scale (1: like very much, 2: like, 3: undecided, 4: do not like, 5: do not like at all) is displayed to subject together with a remainder on the remaining time.

All 3 states are repeated for 60 times to view 60 3D shapes while the minimum time of each trial is set to 14 seconds and the maximum time of each trial is set to 24 seconds, so the time for a subject to complete the experiment is within 14 to 24 minutes.

The acquisition process consists of 3 main factors, the subject, stimuli and acquisition device. The following sub-sections explain the details on the 3 main factors.

The subjects

5 subjects (3 females and 2 males) with an age range of 22-26 (mean=22.8) are involved in the acquisition process in this experiment.

All the subjects are interviewed to ensure there is no history of psychiatric illness and had normal or corrected-to-normal vision. A brief introduction is given to the subjects which includes the aim and the design of the study. The subjects are advised to minimize their movement and not to touch or put their hands on their faces during the whole process acquisition to reduce artifacts on the EEG signals.

3D stimuli

60 3D shapes as shown in Figure-2 are used as stimuli to elicit human aesthetics experience.

The 3D shapes are designed to have a bracelet-like shape which is generated by using the Gielis superformula [21] as shown in (1).

$$r(\theta) = \frac{1}{n1\sqrt{\left(\left|\frac{1}{a}\cos\left(\frac{m}{4}\theta\right)\right|\right)^{n2} + \left(\left|\frac{1}{b}\sin\left(\frac{m}{4}\theta\right)\right|\right)^{n3}}} \quad (1)$$

By multiplying an additional superformula using spherical product as shown in (2), (3) and (4), the generated shapes are extended to 3D.

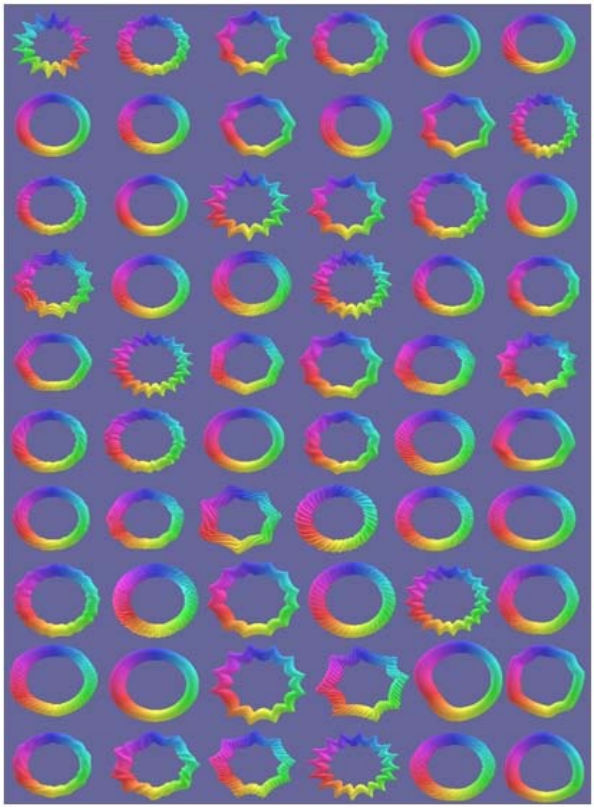

Figure-2. The 3D stimuli used for acquisition.

$$x = r_1(\theta) \times \cos(\theta) \times r_2(\varphi) \times \cos(\varphi) \quad (2)$$

$$y = r_1(\theta) \times \sin(\theta) \times r_2(\varphi) \times \cos(\varphi) \quad (3)$$

$$z = r_2(\varphi) \times \sin(\varphi) \quad (4)$$

where $-\pi \leq \theta < \pi$ and $-\frac{\pi}{2} \leq \varphi < \frac{\pi}{2}$.

To generate 3D shapes with different properties using the Gielis superformula, 10 parameters (m1, n11, n12, n13, m2, m21, m22, m23, c, and t) are required. Most of the parameters to generate the shape are randomized. However, to avoid the generated shape running out of bracelet-like shape, the random values are fixed within a range. The parameter m1, n11, n13, m2, m21, and m23 are fixed at the range from 0 to 20. While for parameters n12 and n22 are fixed at the range from 15 to 30. The parameter c is fixed at the range from 1 to 10 and the parameter t is fixed at 5.5 to maintain the radius of the shapes.

The 3D shapes are virtually displayed on a computer screen with rotation on the shapes to allow subjects to view the shapes at different angles.

Acquisition device

A medical grade wireless EEG device from Advance Brain Monitoring (ABM), B-Alert X10 as shown

in Figure-3(a) with 9 electrodes channels is used to acquire EEG signals from the subjects. The sampling rate of B-Alert X10 is 256Hz with 16 bits.

The electrodes positions (i.e. F3, Fz, F4, C3, Cz, C4, P3, POz and P4) are based on international 10-20 electrode placement system as shown in Figure-3(b) with 2 reference electrodes placed on left and right mastoid bone.

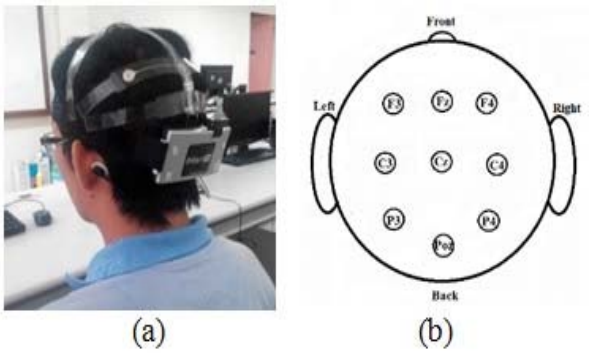

Figure-3. (a) The ABM b-alert X10 headset. (b) Electrode positions of ABM b-alert X10 according to international 10-20 electrode placement system.

SIGNAL PROCESSING AND FEATURE EXTRACTION

Software Development Kits (SDK) of B-Alert X10 which provided by ABM is available in MATLAB. The acquired EEG signals are decontaminated internally by the SDK. The artifacts include EMG (electromyography), eye blinks, excursions, saturations and spikes are removed from the EEG signals, whereas artifacts such as excursions, saturations and spikes in the EEG signals are replaced by zero values. The decontamination algorithm removes environmental artifacts by applying a 60 Hz notch filter, where artifacts such as excursions, saturations and spikes are analyzed in the time domain. The EEG signals are then deconstructed using wavelet transformation to remove EMG and eye blink activities [22]. To remove the zero values, nearest neighbor interpolation (NNI) [23] is then applied to the EEG signals.

5 frequency rhythms include alpha, beta, gamma, theta and delta are interest features in the signals.

The feature extraction is based on Discrete Wavelet Transform (DWT). DWT decomposes EEG signals into approximation coefficients and detailed coefficients. Daubechies' 4 discrete wavelet (db4) wavelet function is used to decomposing EEG signals into 5 levels (see Table-1) to obtain alpha, beta, gamma, theta and delta rhythms. Wavelet function db4 is typically chosen for its near optimal time-frequency localization properties [24].

Table-1. Decomposition of EEG signals.

Frequency Range (Hz)	Decomposition Level	Frequency Bands	Frequency Bandwidth (Hz)
1-4	A5	Delta	4
4-8	D5	Theta	4
8-16	D4	Alpha	6
16-32	D3	Beta	18
32-64	D2	Gamma	32
64-128	D1	Noises	64

Entropy is then calculated for 5 rhythms, alpha, beta, gamma, theta and delta rhythms.

CLASSIFICATION

The classifiers used in this study are Linear Discriminant Analysis (LDA) [25] and K-Nearest Neighbor (KNN) [26] for classifying 2 discrete preferences, like and dislike. An LDA finds the optimal hyper-plane to separate the classes, while KNN classified based on the *k* nearest objects. The nearest neighbor of KNN are tested using different values from 2-10 and the value of 8 which achieved the maximum classification accuracy is selected.

Table-2 shows the training and testing features (F) for each of the subjects. In the training set, the number of data of like and dislike are 79 and 102 respectively. In the testing set, the number of data of like and dislike are 16 and 40 respectively. The total of training data is 181 and the total of testing data is 56.

The Like class refers to trials rated at 4: Like and 5: Like very much. Meanwhile, the Dislike class correspond to the trials rated as 1: do not like at all and 2: do not like. The neutral class corresponding to rating at 3: Undecided, where neutral is not included in the training and testing in classifiers. The ratio of training to testing cases of the data is 3:1.

Table- 2. Training and testing feature.

Subject	Training Set			Testing Set		
	Like F	Dislike F	Total F	Like F	Dislike F	Total F
1	16	14	30	1	8	9
2	11	20	31	1	7	8
3	21	24	45	6	9	15
4	15	17	32	4	7	11
5	16	27	43	4	9	13
Total	79	102	181	16	40	56

RESULTS AND DISCUSSION

The classification accuracy with different combinations of entropy on the rhythms for all electrode channels and all frontal channels (see Table-3).

Table-3. Classification accuracy of LDA and KNN using all channels and all frontal channels.

Entropy of rhythm(s)	All Channels		Fz, POz and P4	
	LDA	KNN	LDA	KNN
α	73.21%	64.29%	69.64%	57.14%
β	62.50%	53.57%	58.93%	60.71%
θ	57.14%	64.29%	58.93%	60.71%
γ	50.00%	62.50%	66.07%	60.71%
δ	73.21%	64.29%	71.43%	58.93%
α γ β	55.36%	60.71%	55.36%	66.07%
β γ	51.79%	57.14%	55.36%	62.50%
α β	53.57%	62.50%	55.36%	58.93%
α β γ δ θ	57.14%	62.50%	58.93%	69.64%
α β γ δ	53.57%	58.93%	57.14%	64.29%
α θ	60.71%	62.50%	57.14%	62.50%
γ θ	55.36%	62.50%	55.36%	57.14%
θ δ	60.71%	62.50%	58.93%	60.71%
α γ β θ	53.57%	64.29%	58.93%	53.57%
β γ θ	46.43%	60.71%	55.36%	53.57%
α β θ	50.00%	71.43%	57.14%	57.14%
α γ θ	60.71%	67.86%	55.36%	60.71%
β θ	51.79%	60.71%	57.14%	53.57%
γ θ δ	50.00%	62.50%	60.71%	64.29%
α γ	60.71%	62.50%	62.50%	57.14%
α δ θ	60.71%	57.14%	58.93%	60.71%
α β δ θ	55.36%	64.29%	60.71%	66.07%
β δ θ	53.57%	64.29%	57.14%	64.29%
α δ	67.86%	57.14%	66.07%	62.50%
β γ δ θ	51.79%	62.50%	57.14%	64.29%

where α represents alpha, β represents beta, θ represents theta, γ represents gamma, and δ represents delta rhythm bands respectively.

The highest accuracy for using rhythms from all channels is 73.21% by using LDA with the entropy of the alpha rhythm. The lowest accuracy for using rhythms from all channels is 46.43% using LDA with the entropy of the beta, theta and gamma rhythms. The performance of KNN is better than LDA with mean accuracies of 62.13% and 57.29% respectively.

The accuracies of using entropy from all the frontal rhythms range from 55.36% to 71.43%. The highest accuracy for rhythms from all frontal channels is 71.43% by using LDA with the entropy of the delta rhythm. The performance of KNN is better than LDA with mean accuracies of 60.57% and 59.43% respectively.

The left and right frontal activities are related with emotion where the left frontal activation is related with positive emotion while the right frontal activation is related with negative emotion [26]. The left and right frontal channels are channels F3 and F4 respectively. Channel F3 was selected based on [14], which showed prefrontal cortex activities is related to aesthetics experiences. The classification accuracy using different frontal lobe is as shown in Table-4.

Table-4. Classification accuracy of LDA and KNN using different frontal lobe channels.

Entropy of rhythm(s)	F3 and F4		F3	
	LDA	KNN	LDA	KNN
α	71.43%	51.79%	71.43%	58.93%
β	64.29%	57.14%	71.43%	67.86%
θ	69.64%	57.14%	69.64%	58.93%
γ	71.43%	66.07%	71.43%	67.86%
δ	71.43%	64.29%	71.43%	53.57%
α γ β	57.14%	64.29%	60.71%	66.07%
β γ	55.36%	62.50%	62.50%	60.71%
α β	62.50%	60.71%	71.43%	66.07%
α β γ δ θ	53.57%	64.29%	66.07%	75.00%
α β γ δ	55.36%	57.14%	62.50%	66.07%
α θ	67.86%	66.07%	67.86%	57.14%
γ θ	66.07%	60.71%	69.64%	66.07%
θ δ	69.64%	58.93%	67.86%	64.29%
α γ β θ	53.57%	69.64%	66.07%	73.21%
β γ θ	55.36%	67.86%	66.07%	64.29%
α β θ	60.71%	66.07%	67.86%	62.50%
α γ θ	64.29%	62.50%	67.86%	75.00%
β θ	60.71%	58.93%	69.64%	66.07%
γ θ δ	67.86%	57.14%	67.86%	64.29%
α γ	71.43%	64.29%	71.43%	67.86%
α δ θ	69.64%	67.86%	67.86%	66.07%
α β δ θ	58.93%	66.07%	67.86%	73.21%
β δ θ	60.71%	62.50%	67.86%	69.64%
α δ	71.43%	58.93%	71.43%	66.07%
β γ δ θ	58.93%	62.50%	66.07%	73.21%
β δ θ	60.71%	62.50%	67.86%	69.64%
α δ	71.43%	58.93%	71.43%	66.07%
β γ δ θ	58.93%	62.50%	66.07%	73.21%

where α represents alpha, β represents beta, θ represents theta, γ represents gamma, and δ represents delta rhythm bands respectively.

Using the entropy from channels F3 and F4 yielded accuracies that ranged from 53.57% to 71.43% with LDA while 51.79% to 69.64% was obtained with KNN. From the observations, the accuracy of using the entropy from all the frontal channels does not shows any improvements compared to the other channels.

Meanwhile, the use of the entropy from the F3 channel yielded an accuracy of up to 75% by using the entropy of all the interested rhythms and also the entropy of the alpha, gamma and theta rhythms with KNN. The lowest accuracy is 53.57% by using the entropy of the delta rhythm with KNN.

From the observations, classifications based on combinations of channels at the parietal and frontal lobes especially Fz, POz and P4 achieved an accuracy of up to 82.14%. The combinations of channels from the frontal and parietal lobes which achieved the minimum accuracy of 78.57% are as shown in Tables-5 and 6.

Table-5. Classification accuracy of LDA and KNN using channel POz and P4, and Fz and POz.

Entropy of rhythm(s)	POz and P4		Fz and POz	
	LDA	KNN	LDA	KNN
α	71.43%	66.07%	73.21%	78.57%
β	71.43%	67.86%	62.50%	60.71%
θ	69.64%	66.07%	62.50%	64.29%
γ	71.43%	62.50%	69.64%	64.29%
δ	66.07%	62.50%	71.43%	67.86%
α γ β	78.57%	66.07%	60.71%	66.07%
β γ	71.43%	62.50%	58.93%	57.14%
α β	73.21%	67.86%	62.50%	64.29%
α β γ δ θ	75.00%	69.64%	60.71%	60.71%
α β γ δ	76.79%	62.50%	64.29%	64.29%
α θ	69.64%	58.93%	69.64%	62.50%
γ θ	71.43%	67.86%	60.71%	66.07%
θ δ	66.07%	64.29%	67.86%	73.21%
α γ β θ	75.00%	64.29%	55.36%	64.29%
β γ θ	69.64%	66.07%	53.57%	66.07%
α β θ	67.86%	62.50%	58.93%	64.29%
α γ θ	71.43%	64.29%	67.86%	66.07%
β θ	67.86%	73.21%	57.14%	64.29%
γ θ δ	69.64%	67.86%	71.43%	73.21%
α γ	73.21%	71.43%	71.43%	69.64%
α δ θ	67.86%	58.93%	71.43%	67.86%
α β δ θ	64.29%	62.50%	60.71%	60.71%
β δ θ	64.29%	66.07%	57.14%	71.43%
α δ	71.43%	55.36%	71.43%	57.14%
β γ δ θ	66.07%	67.86%	53.57%	71.43%

where α represents alpha, β represents beta, θ represents theta, γ represents gamma, and δ represents delta rhythm bands respectively.

The use of the entropy from channels POz and P4 yielded accuracies that ranged from 64.29% to 78.57% using LDA and 55.36 to 73.21% for KNN. The highest accuracy is 78.57% which was obtained using the entropy of the alpha, gamma and beta rhythms using LDA, while the lowest accuracy is 55.36% which was obtained using the entropy of the alpha and delta rhythms with KNN.

The use of the entropy from channels Fz and POz yielded an accuracy of up to 78.57% using the entropy of the alpha rhythm with KNN. The use of LDA to classify the entropy from channels Fz and POz obtained accuracies that ranged from 53.57% to 73.21% and the use of KNN to classify the entropy from channels Fz and POz obtained accuracies that ranged from 57.14% to 78.57%. The lowest accuracy is 53.57% which was obtained using the entropy of the beta, gamma and theta rhythms using LDA.

Table-6. Classification accuracy of LDA and KNN using channel Fz and P4, and Fz, POz and P4.

Entropy of rhythm(s)	Fz and P4		Fz, POz and P4	
	LDA	KNN	LDA	KNN
α	66.07%	64.29%	73.21%	67.86%
β	58.93%	60.71%	60.71%	57.14%
θ	64.29%	64.29%	62.50%	60.71%
γ	67.86%	57.14%	69.64%	73.21%
δ	73.21%	69.64%	66.07%	73.21%
α γ β	62.50%	69.64%	67.86%	62.50%
β γ	62.50%	55.36%	66.07%	60.71%
α β	57.14%	64.29%	60.71%	64.29%
α β γ δ θ	60.71%	78.57%	66.07%	69.64%
α β γ δ	66.07%	76.79%	66.07%	67.86%
α θ	60.71%	58.93%	73.21%	64.29%
γ θ	58.93%	64.29%	62.50%	62.50%
θ δ	67.86%	78.57%	62.50%	71.43%
α γ β θ	57.14%	64.29%	62.50%	55.36%
β γ θ	58.93%	66.07%	60.71%	62.50%
α β θ	55.36%	64.29%	53.57%	57.14%
α γ θ	55.36%	58.93%	66.07%	58.93%
β θ	58.93%	67.86%	57.14%	60.71%
γ θ δ	64.29%	69.64%	58.93%	78.57%
α γ	62.50%	64.29%	71.43%	64.29%
α δ θ	67.86%	71.43%	69.64%	67.86%
α β δ θ	55.36%	76.79%	60.71%	67.86%
β δ θ	57.14%	78.57%	62.50%	78.57%
α δ	71.43%	58.93%	73.21%	66.07%
β γ δ θ	66.07%	80.36%	64.29%	82.14%

where α represents alpha, β represents beta, θ represents theta, γ represents gamma, and δ represents delta rhythm bands respectively.

The use of the entropy from channels Fz and P4 achieved accuracies that ranged from 55.36% to 73.21% using LDA and 55.36% to 80.36% using KNN. The highest accuracy is 80.36% which was obtained using the entropy of the beta, gamma, theta and delta rhythms. Meanwhile, a high accuracy of 78.57% was obtained through using the entropy of all the rhythms, the entropy of the theta and delta rhythms, and also the entropy of the beta, theta and delta rhythms.

Meanwhile, the use of the entropy from channels Fz, POz and P4 achieved accuracies that ranged from 53.57% to 73.21% using LDA and 55.36% to 82.14% using KNN. The highest accuracy is 82.14% which was obtained using the entropy of the beta, theta and delta rhythms, whereas an accuracy of 78.57% was obtained using the entropy of the gamma, theta and delta rhythms with KNN and also the beta, theta and delta rhythms with KNN. Furthermore, the lowest accuracy is 53.21% which was obtained using the entropy of the alpha, beta and theta rhythms with LDA.

The confusion matrix of the like class of the highest accuracy of 82.14% is as shown in Table-7.

Table-7. Confusion matrix on the highest accuracy obtained.

	Like (predicted)	Dislike (predicted)
Like (actual)	10	6
Dislike (actual)	4	36

The total testing data were 56, the number of true positive, false negatives, false positives and true negatives were 10, 6, 4 and 36 respectively.

The entropy of rhythms from Fz, POz and P4 are informative in a way that the combination achieved an accuracy of 78.57% and above. This is probably because of the dorsal pathway involve parietal lobe and channel POz, where channel POz is also known as parieto-occipital midline which believed to involve in processing 3D shapes from motion [27]. Meanwhile, both the parietal and frontal lobes are believed to be involved in directing attention to spatial location, especially the right parietal lobe [28].

CONCLUSIONS

This study investigated the preference of human subjects on 3D abstract shapes using an EEG acquisition device to capture brain signals.

The ABM B-Alert X10 device with 9 electrode channels was used as acquisition device. DWT technique is then applied to obtain alpha, beta, gamma, theta and delta rhythms. Then the entropy of the rhythms was calculated for each of the rhythms. LDA and KNN classifiers were used to train and test the system using different combination of rhythms and channels.

The highest accuracy obtained was 82.14% using the entropy of the beta, gamma, theta and delta rhythms of channel Fz, POz and P4 with KNN, where the use of the entropy from the combination of channels Fz, POz and P4 were able to achieve an accuracy of 78.57% and above. The results suggest that channels POz, P4 and Fz were more informative in classifying human visual preference in 3D.

In future, we plan to develop a real-time human visual preference detection system in 3D.

ACKNOWLEDGEMENTS

This project is supported through the research grant ref: FRGS/2/2013/ICT02/UMS/02/1 from the Ministry of Education, Malaysia.

REFERENCES

[1] B. Chawda, B. Craft, P. Cairns, S. Rüger and D. Heesch. September 2005. Do Attractive Things Work Better? An Exploration of Search Tool Visualisations. In Proceedings of 19th British HCI Group Annual Conference (HCI2005), Edinburgh, UK. L. McKinnon, O. Bertelsen, and N. Bryan-Kinns (Eds). pp. 1-4.

[2] S. Brown and E. Dissanayake. 2009. The arts are more than aesthetics: Neuroaesthetics as narrow aesthetics. In Neuroaesthetics. M. Skov and O. Vartanian (Eds). pp. 43-57.

[3] G. M. Aurup and A. Akgunduz, July 2012. Preference Extraction from EEG: An Approach to Aesthetic Product Development. In Proceedings of the 2012 International Conference on Industrial Engineering and Operations Management, Istanbul, Turkey. pp. 1178-1186.

[4] J. Prinz, Emotion and aesthetic value. 2011. The Aesthetic Mind: Philosophy and Psychology: Oxford University Press. E. Schellekens and P. Goldie (Eds). pp. 71-88.

[5] S. K. Hadjidimitriou and L. J. Hadjileontiadis, 2013. EEG-Based Classification of Music Appraisal Responses Using Time-Frequency Analysis and Familiarity Ratings. IEEE Trans. Affective Computing, Vol. 4, No. 2, pp. 161-172.

[6] Y. Kim, K. Kang, H. Lee, and C. Bae. 2015. Preference Measurement Using User Response Electroencephalogram. Springer Berlin Heidelberg. Computer Science and its Applications. pp. 1315-1324.

[7] J. Moon, Y. Kim, H. Lee, C. Bae, and W. C. Yoon. 2013. Extraction of User Preference for Video Stimuli Using EEG-Based User Responses, ETRI Journal, Vol. 35, No. 6, pp. 1105-1114.

[8] T. Love. 2013. Design and sense: implications of Damasio's neurological findings for design theory. Proceedings of Science and Technology of Design, Senses and Sensibility in Technology-Linking Tradition to Innovation through Design, pp. 25-26, Lisbon, Portugal.

[9] M. Li, B. L. Lu. 2009. Emotion classification based on gamma-band EEG. Engineering in Medicine and Biology Society: Annual International Conference of the IEEE: EMBC 2009, pp. 1223-1226.

[10] M. Murugappan, S. Murugappan, and C. Gerard. 2014, March. Wireless EEG signals based neuromarketing system using Fast Fourier Transform (FFT). Signal Processing & its Applications (CSPA) on 2014 IEEE 10th International Colloquium, pp. 25-30.

[11] X. W. Wang, D. Nie, and B. L. Lu. January 2011. EEG-based emotion recognition using frequency domain features and support vector machines. Neural Information Processing. Vol. 7062, pp. 734-743.

[12] Y. Liu, O. Sourina, and M. K. Nguyen. October 2010. Real-time EEG-based human emotion recognition and

visualization. IEEE Trans. International Conference on Cyberworlds (CW). pp. 262-269.

[13] C. Brown, A. B. Randolph, and J. N. Burkhalter. 2012. The Story of Taste: Using EEGs and Self-Reports to Understand Consumer Choice. The Kennesaw Journal of Undergraduate Research. Vol. 2, No. 1, p. 5.

[14] C. J. Cela-Conde, G. Marty, F. Maestú, T. Ortiz, E. Munar, A. Fernández, M. Roca, J. Rosselló, F. Quesney. 2004. Activation of the prefrontal cortex in the human visual aesthetic perception. Proceedings of the National Academy of Sciences of the United States of America. Vol. 101, No. 16, pp. 6321-6325.

[15] B. R. Cottereau, S. P. McKee, and A. M. Norcia. 2014. Dynamics and cortical distribution of neural responses to 2D and 3D motion in human. Journal of neurophysiology. Vol. 111, No. 3, pp.533-543.

[16] J. T. Todd. 2004. The visual perception of 3D shape. Trends in cognitive sciences. Vol. 8, No. 3, pp. 115-121.

[17] S. E. Palmer, K. B. Schloss, and J. Sammartino. 2013. Visual aesthetics and human preference. Annual review of psychology. Vol. 64, pp. 77-107.

[18] H. Takagi. 2001. Interactive evolutionary computation: Fusion of the capabilities of EC optimization and human evaluation. Proceedings of the IEEE. Vol. 89, No. 9, pp. 1275-1296.

[19] V. J. Shackleton. 1981. Boredom and repetitive work: a review. Personnel Review. Vol. 10, No. 4, pp. 30-36.

[20] A. Craig, Y. Tran, N. Wijesuriya, and H. Nguyen. 2012. Regional brain wave activity changes associated with fatigue. Psychophysiology, Vol. 49, No. 4, pp. 574-582.

[21] J. Gielis. 2003. A generic geometric transformation that unifies a wide range of natural and abstract shapes. American journal of botany, Vol. 90, No. 3, pp. 333-338.

[22] C. Berka, D. J. Levendowski, M. N. Lumicao, A. Yau, G. Davis, V. T. Zivkovic, R. E. Olmstead, P. D. Tremoulet and P. L. Craven, P. 2007. EEG correlates of task engagement and mental workload in vigilance, learning, and memory tasks. Aviation, space, and environmental medicine, 78(Supplement 1): B231-B244.

[23] D. Garcia. 2010. Robust smoothing of gridded data in one and higher dimensions with missing values. Computational Statistics & Data Analysis. Vol. 54, No. 4, pp. 1167-1178.

[24] M. Murugappan, N. Ramachandran, Y. Sazali. 2010. Classification of human emotion from EEG using discrete wavelet transform. Journal of Biomedical Science and Engineering. Vol. 3, pp. 390-396.

[25] J. Ye, R. Janardan, and Q. Li. 2005. Two-Dimensional Linear Discriminant Analysis. Advances in Neural Information Processing Systems. pp. 1569-1576.

[26] Y. Song, J. Huang, D. Zhou, H. Zha, and C. L. Giles. 2007. Iknn: Informative k-nearest neighbor pattern classification. Knowledge Discovery in Databases: PKDD 2007, Springer Berlin Heidelberg, pp. 248-264.

[27] A. L. Paradis, V. Cornilleau-Peres, J. Droulez, P. F. Van De Moortele, E. Lobel, A. Berthoz, D. Le Bihan and J. B. Poline. 2000. Visual perception of motion and 3-D structure from motion: an fMRI study. Cerebral Cortex. Vol. 10, No. 8, pp. 772-783.

[28] G. Pourtois, Y. Vandermeeren, E. Olivier, and B. De Gelder. 2001. Event-related TMS over the right posterior parietal cortex induces ipsilateral visuo-spatial interference. Neuroreport, Vol. 12, No. 11, pp. 2369-2374.